

Analysis of electrochemical noise in NiCd batteries throughout their lifetime

Burak ÜLGÜT*

Department of Chemistry, Faculty of Science, Bilkent University, Ankara, Turkey

Received: 01.11.2017

Accepted/Published Online: 02.04.2018

Final Version: 01.06.2018

Abstract: Electrochemical noise measurements have been applied to electrochemical systems that show stochastic behavior. The standard area of study that benefits from this stochastic analysis is localized corrosion modes like pitting and crevice corrosion. Application of electrochemical noise measurements to battery systems, though rare, is recently becoming more popular. The present contribution first establishes a method of analyzing electrochemical voltage noise data for NiCd batteries, then follows four samples of batteries in terms of voltage noise throughout their lifetimes. The noises exhibited by battery systems are small, but finite. This noise is expected to be due to variations in the electrochemistry on the electrode surfaces of the battery. After careful analysis, the voltage noise behavior of NiCd batteries does not appear to show a statistically significant variation of electrochemical voltage noise throughout their lifetimes.

Key words: Battery, electrochemical noise, NiCd, power supply noise

1. Introduction

Electrochemical noise (EN) measurements have been employed in the literature in order to study events that are stochastic in nature. Particularly in the field of electrochemical corrosion, two stochastic events dominate under certain conditions: crevice corrosion and pitting corrosion. Techniques developed for uniform corrosion analysis such as Tafel and polarization resistance cannot be employed in studies of stochastic processes. The details of stochastic events have to be measured using techniques that measure the system in all its details as a function of time and then develop methods of analysis to correlate the properties of the stochastic events to the details of the measured voltage and noise signals.

Noise methods in electrochemistry date back to 1968 when Barker laid the theoretical foundations for noise due to electrochemical processes.¹ This report inspired numerous experimental studies within the next few decades. Some of the most noteworthy include a report on a measurement method by Blanc et. al.² and the report by Hladky and Dawson in 1980 that tied electrode noise to localized corrosion processes.³ The latter report in particular was one of the pioneering efforts in laying the foundations for a method to measure the details of localized corrosion that is known to be stochastic in nature. This was a crucial step in the analysis of localized corrosion that cannot be investigated using standard methods developed to investigate uniform corrosion. This led to a large body of research on localized corrosion employing noise-based methods. Though a thorough review of EN-based corrosion studies is beyond the scope of the present manuscript, some prominent examples will be mentioned. In 1993, Mansfeld and Xiao⁴ reported on the use of noise-based methods to follow iron electrodes corroding in chloride solutions, which induce pitting and crevicing. In 1995, Legat and

*Correspondence: ulgut@fen.bilkent.edu.tr

Doleček⁵ reported on studies of stainless steel electrodes, again detailing the localized corrosion processes using EN measurements. In 1998, Roberge and Lenard⁶ reported on EN and impedance studies of localized corrosion on aluminum alloys.

Noise measurements in the field of corrosion have been controversial in terms of their analyses, but there is wide agreement among researchers in the literature that EN measurements accurately reflect stochastic processes in the system.

Various analysis methods have been developed for EN methods. The most common way to analyze EN data is by inspecting the frequency domain components of the data. This is typically done using a fast Fourier transform (FFT) algorithm. The details of the application of FFT algorithms and how the resulting information in the frequency domain is processed were nicely reviewed in a paper by Cottis.⁷ More recently, analysis more suitable for nonperiodic time traces was developed. Wavelet analyses⁸ are applied and used successfully in the analyses of EN data. Most recently, in 2016, Cottis and coworkers investigated the relationship between wavelet and FFT methods of analyzing EN data.⁹ The report showed that the two methods can be correlated through simple relationships and that either method can be used. The stochastic process detector (SPD) is another method developed for analyzing nonrepetitive EN data. The SPD was developed and detailed by Roberge.¹⁰

Noise measurements of batteries have been sporadic in the literature. To the author's knowledge, the earliest example was reported within a noise analysis of a device that was battery powered.¹¹ In this report, the noise behaviors of two different 9-V battery constructions were compared under different applied currents. The noise level was measured by using various resistor battery connection architectures in order to compare the noise levels of two constructions. Later in 1989 a report by Roberge et al.¹² investigated the voltage noise behavior of sealed lead acid type batteries under applied load. By adding an RC filter into the measurement loop for the voltage, the bandwidth was constricted to the desired value and the measured noise levels clearly indicated electrolysis, which is detrimental to the life of the battery. In a paper published in 1999¹³ similar behavior was observed for a number of other different aqueous electrolyte-based batteries based on Ni chemistry. Later in 2003 lead acid batteries from a single manufacturer were investigated in order to check for using voltage noise as an indicative tool to follow battery state of health.¹⁴ Though there appears to be some correlation, the statistical significance of the noisy data presented is suspect given the reported variance of the data. Most recently, a report from researchers at the University of Poitiers and collaborators¹⁵ reported measurements with very low backgrounds. Their analysis relied on the measurement of noise power as a function of state of charge. However, the reported trends in the total noise power clearly suffer from a lack of detrending. Without proper detrending, the total power in the data appears to be larger wherever the V vs. t curve displays a high slope.

One important area where batteries are typically used is for analytical measurement tools that are designed to be low-noise. Since DC power obtained via rectification of AC power is always prone to ripples, battery power is preferred for low-noise applications.¹⁶ In this case, the changes of the noise level as the battery goes through its life is of utmost importance.

For this application, nickel-cadmium type batteries are typically used due to their safe aqueous chemistry and stable voltage levels (e.g., Manual for the Low Noise 1201 Voltage Preamplifier from DL Instruments (Brooktondale, NY), <http://dlinstruments.com/wp-content/uploads/2013/04/1201.pdf>). The present manuscript investigates the apparent noise levels of a NiCd battery system throughout its lifetime.

2. Results and discussion

2.1. Fresh battery and background comparison

As control measurements, voltage noise was measured across a copper wire and a 10-mF capacitor. By playing with the contacts, the copper wire was made to measure $\sim 20\text{ m}\Omega$, which is the measured internal resistance of the battery, and the 10-mF capacitance is seen to have similar impedance magnitudes as the battery. As shown in the impedance spectra in Figure 1, 10 mF and 20 m Ω combined are good negative controls. The expected thermal noise from a resistor of 20 m Ω is roughly $20\text{ pV}/\sqrt{\text{Hz}}$ ($\sqrt{4k_BTR}$), which is clearly below the instrumental noise measured; therefore, the thermal noise is not expected to be the dominant factor. This baseline measurement, compared to a fresh NiCd cell in the charged state, is shown in Figure 1 in the different ways that will be employed throughout the rest of the manuscript. Figure 1 (top) shows the piecewise linear detrended time domain data plotted vs. time. On the left, shown in red is the voltage noise of the shorted lead system, and on the right, in blue, is the voltage noise measured with the battery connected to the measurement system. At the bottom, two analyses are provided. On the bottom left, the frequency domain data are presented with the blue trace showing the noise response of the battery compared to the red trace showing the response of the shorted lead. Lastly, on the bottom right, histograms are presented in the color code used above. In all representations, the measured noise with the battery connected is significantly and verifiably above the noise measured with the shorted lead.

The noise behavior also shows some more interesting features. First, the data are clearly weighted more heavily towards more positive potentials. Though this can be spotted in the time domain representation by the trained eye, it is much easier to notice in the histogram. The peak has a much heavier tail on the positive side compared to the negative side. This indicates that most of the noise-generating processes do so in the direction of increasing voltage. Second, in the frequency domain, the noise behavior of the shorted lead and the battery is clearly the same once the frequency is above $\sim 1\text{ Hz}$. The only differences are in the region of frequencies that are below 1 Hz. This indicates that the apparent noise processes are mostly different in the slower region. The frequencies above 1 Hz are not relevant in measuring any battery-related voltage noise.

2.2. Battery noise vs. state of charge

The next set of experiments involved checking for differences in the noise behavior of the battery as a function of state of charge. For these experiments, the batteries were discharged successively to different potentials and held at the selected potentials for 2 h to ensure equilibration. After equilibration, the voltage was measured and analyzed. The results are presented in Figure 2.

As shown in Figure 2, no significant difference is observed across the entire voltage range of the battery. In both the frequency domain and the histogram, the data show features that do not have any significant differences. It is clear that voltage noise measured is not a function of the state of charge.

2.3. Cycling behavior

All batteries were cycled to their end of life (battery end of life is typically defined as when the battery only has 80% of the original capacity) and beyond. The normalized charge and discharge amounts are shown in Figure 3. In all cases, the charges were normalized to the charge in the initial cycle.

Though all four batteries were bought at the same time from the same wholesaler, they had distinctly different cycling behavior. This is evidence of the variability of battery systems. It is clear that all batteries lose capacity upon cycling to varying degrees. Therefore, the reported results from now on will always report the data on all four batteries in order to ascertain proper statistics.

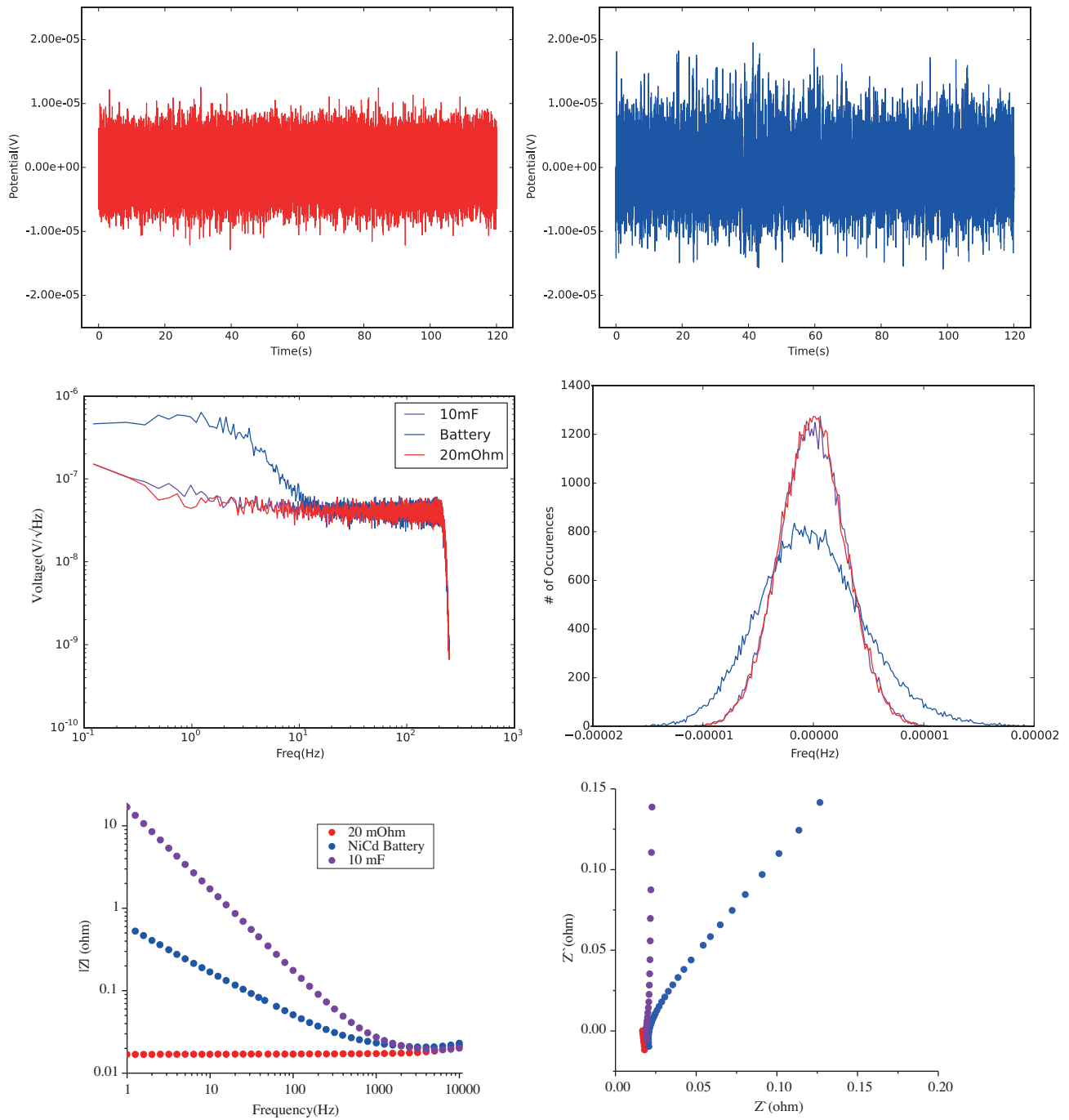


Figure 1. Comparison of the voltage noise of 20 mΩ and the battery. Top, detrended data compared in the time domain: left, top) 20 mΩ; right, top) the battery. For clarity, 10 mF is not shown in the time domain. Middle row displays the noise data in the frequency domain on the left and as a histogram on the right. Bottom, impedance spectra of the battery, 20 mΩ and 10 mF as systems with similar impedance levels shown as Bode (left) and Nyquist (right) plots.

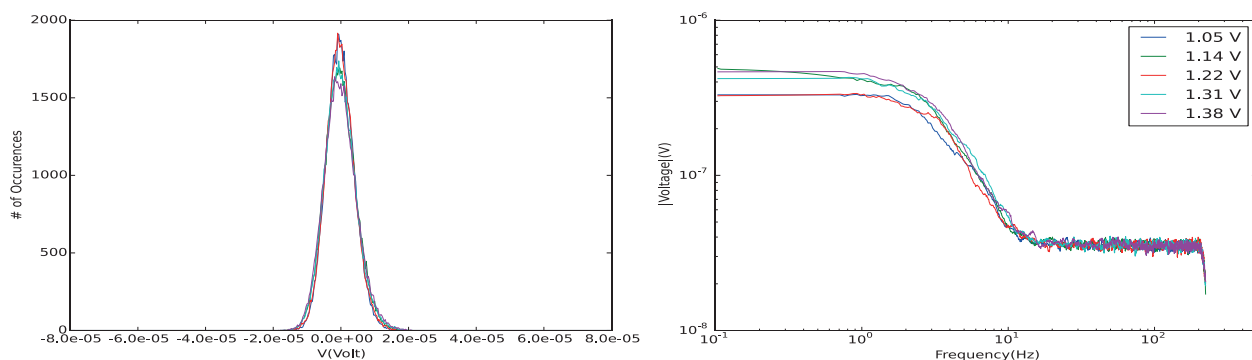


Figure 2. Voltage noise behavior as a function of the state of charge as shown in histogram form on the left and frequency domain form on the right.

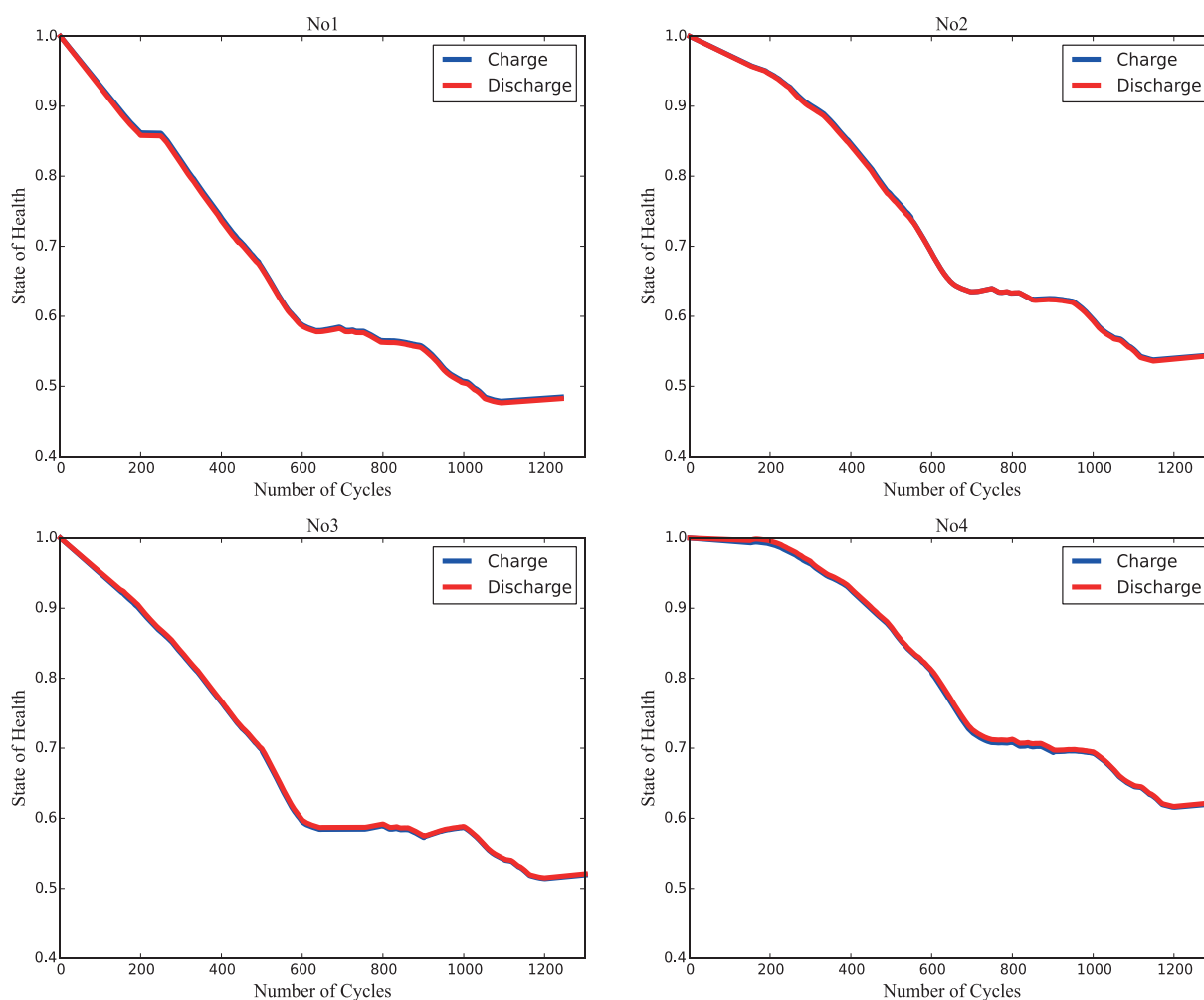


Figure 3. Charge–discharge cycling of 4 samples of the NiCd batteries. In all cases, the amount of charge is normalized to the amount of charge in the first cycle.

Throughout the cycling, batteries were disconnected from the cycler periodically in order to follow the noise behavior. All four batteries were followed independently from each other. The noise behavior in the frequency domain is shown in Figure 4. Though certain small differences in the low frequency region appear, a

careful examination shows no clear trend that significantly indicates a difference. In order to further show this fact, it is worth looking at two additional different plots. Figure 5 shows the total noise power (as a root mean square value) and Figure 6 shows the noise power at 1 Hz as functions of cycle number.

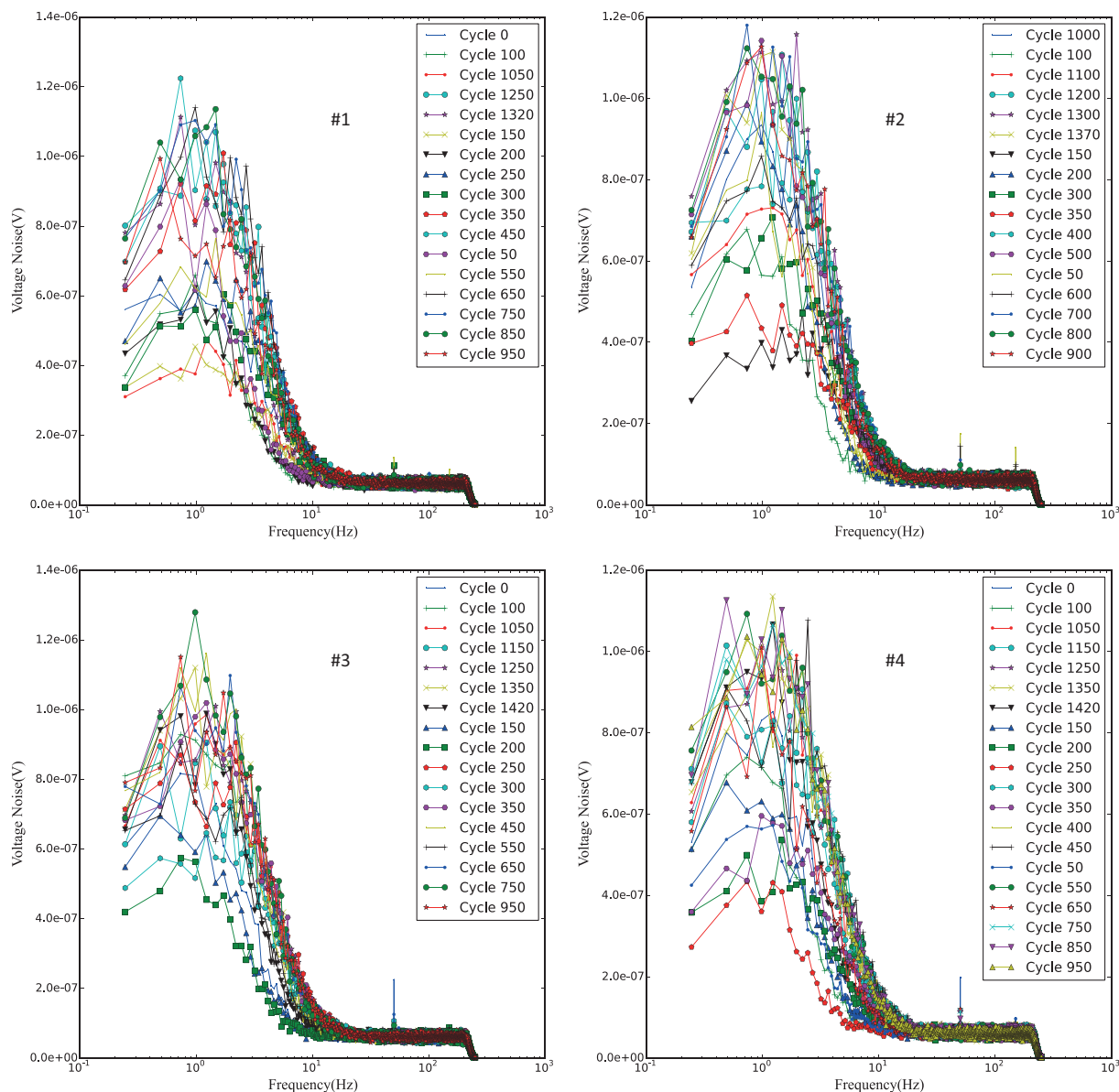


Figure 4. Frequency dependence (in $V/\sqrt{\text{Hz}}$) of the noise behavior of four batteries at various stages of cycling.

In all samples and across the entire lifetime of the battery, no significant change occurs in the voltage noise behavior. Any small change that is possibly visible is both clearly not statistically significant given the standard deviations shown and not reproduced in the other samples.

The data can be displayed in histogram form to check for differences as well. Figure 7 shows the same data analyzed in Figures 4–6 in histogram form. The histograms do not show any significant trend, either. Any variation is not only too small to be statistically significant, but also not reproduced by the other cells that are tested.

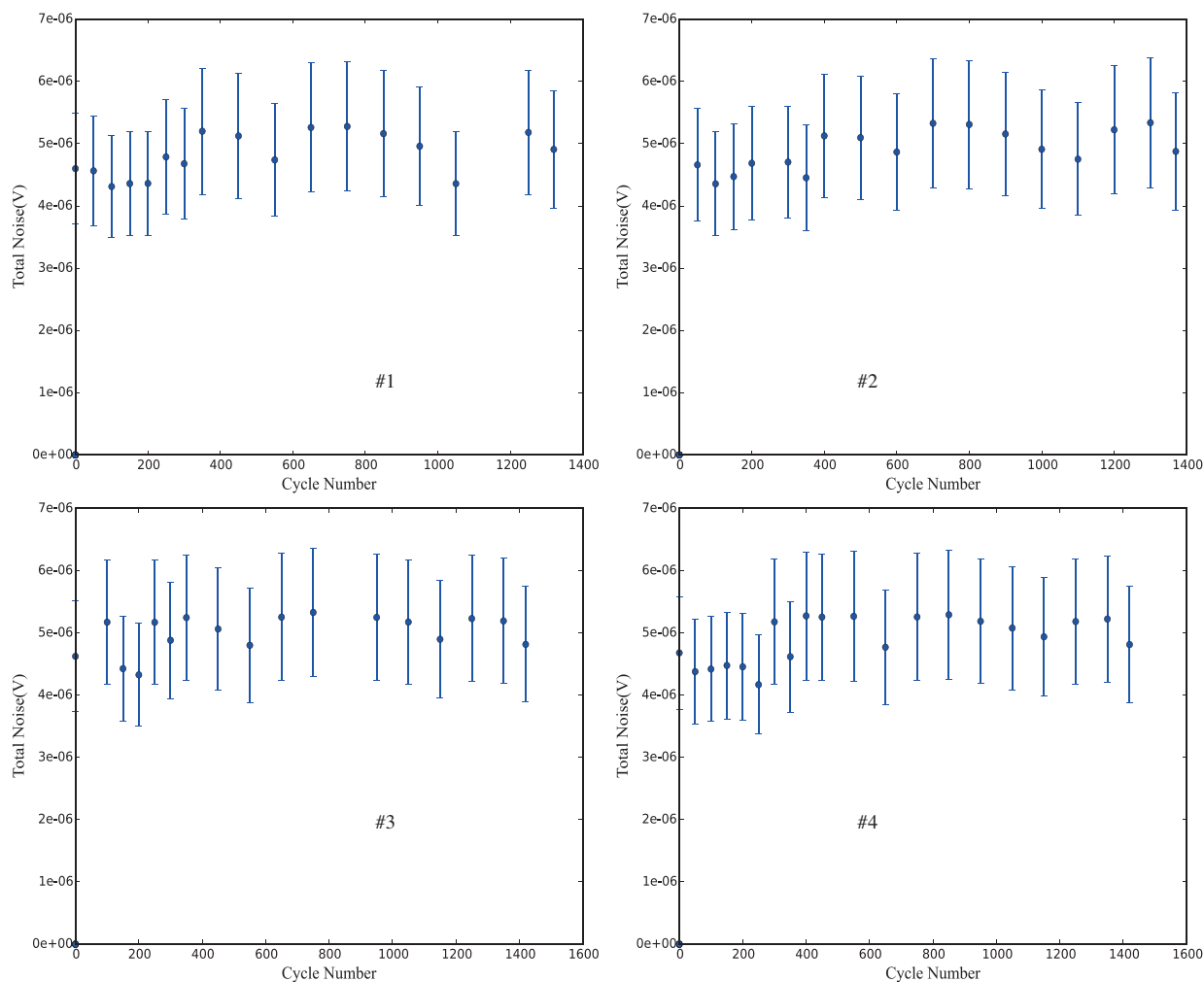


Figure 5. Square root of total noise power (in V) as a function of cycle number for the four battery samples.

It is clear that the apparent noises in the NiCd battery systems are not displaying significant variation throughout their lifetime.

3. Conclusion

The noise levels of NiCd batteries do not significantly change throughout the life of the batteries. The noise measured, though low, is finite and above what is measured on a typical resistor of similar values to the internal impedance of the batteries.

This lack of change further implies that voltage noise levels cannot be used as a significant indicator of battery state of charge or state of health.

4. Experimental

4.1. Materials

The NiCd cells used were manufactured by TNL Technologies (4/5SC) and purchased from local wholesalers. In order to achieve proper statistics on the measurements, four samples of the batteries that were bought out of the same batch at the same time were employed.

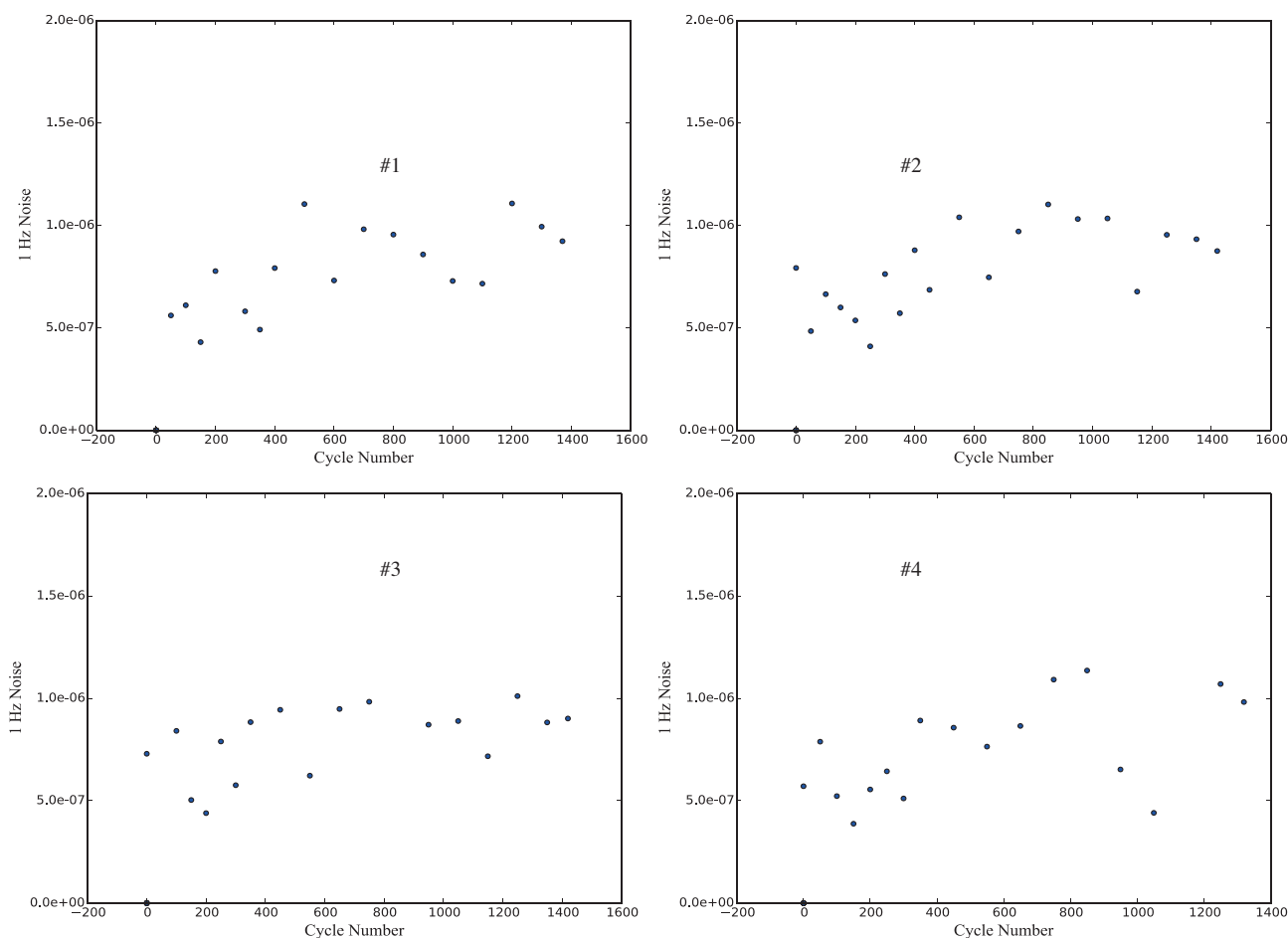


Figure 6. Noise at 1 Hz (in $V/\sqrt{\text{Hz}}$) as a function of cycle number for the four battery samples.

4.2. Measurements

The charge/discharge cycling was performed using Neware BTS4000-5V6A-8CH. All noise measurements were performed using a Gamry Reference 5000E under open circuit potential in an earth-grounded Faraday cage.

Batteries were cycled at 22 mA with potential limits of 1.0 V and 1.4 V. At every 50–100 cycles, the batteries were disconnected from the cycler and connected to the Reference 5000E for noise measurements. Noise measurements were collected for 120 s at a sampling frequency of 500 Hz. This was selected as the sampling frequency since a hardware filter with cutoff of 1000 Hz was in place.

5. Data analysis

The literature contains numerous ways to analyze noise data as reviewed in the introduction. In the current study, the methods that are presented are FFT and histogram analysis. Fourier transforms were visualized in three different ways: a Bode plot showing the magnitude at a given frequency as a function of log frequency, the total noise power across the spectrum as a function of cycle number, and the noise power at 1 Hz as a function of cycle number.

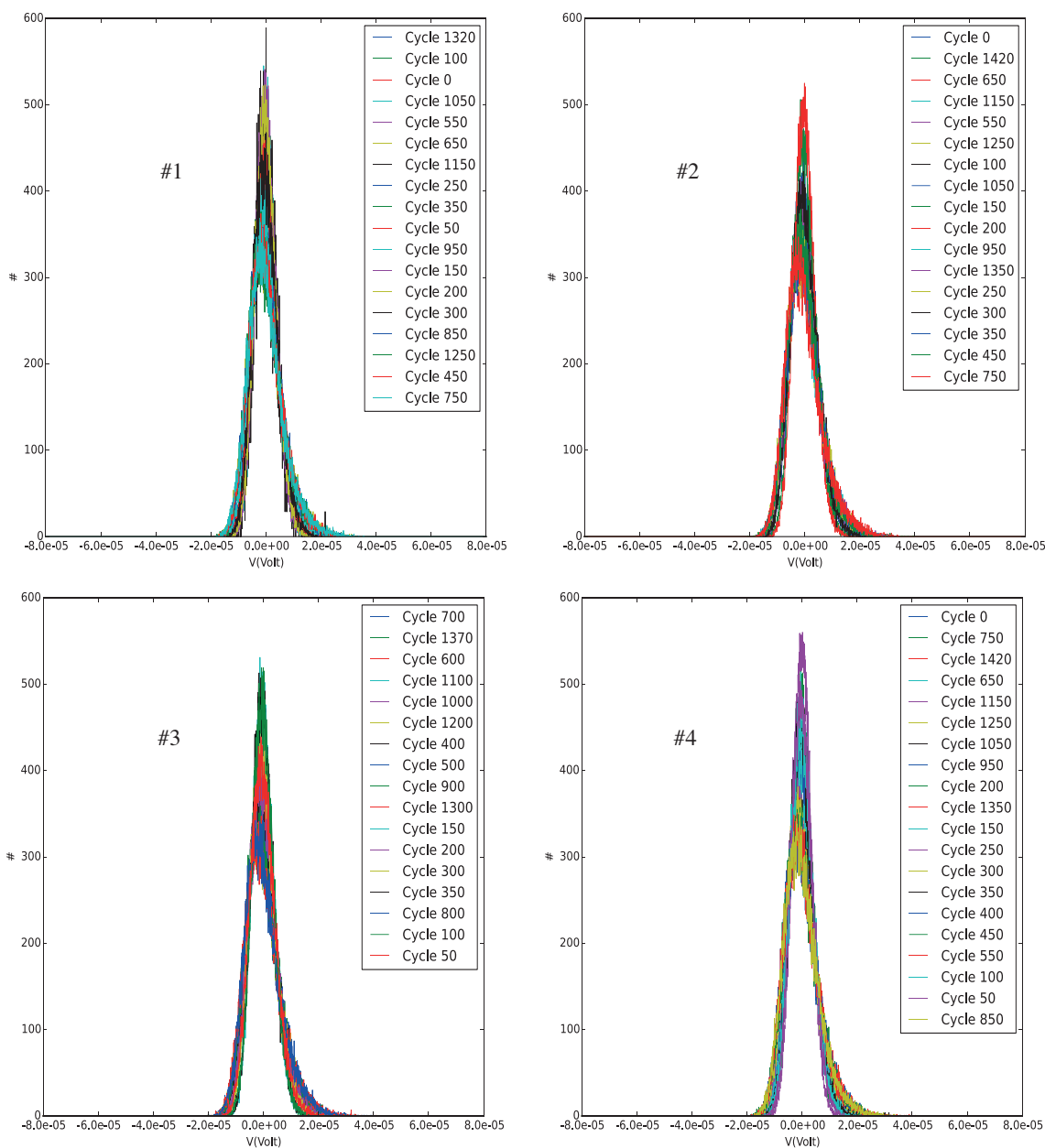


Figure 7. Noise data as a function of cycle number shown as histograms of the observed voltage.

One important part of EN analyses is detrending. Before calculating any frequency domain behavior of the stochastic events, the slow-moving part of the data needs to be properly subtracted out.¹⁷ In batteries, events such as self-discharge have a time constant of ~ 72 h, which is much longer than typical timescales relevant to noise measurements.

Fourier analysis was performed on the data in a piecewise manner. Since the data were collected with 500-Hz sampling rate through 120 s, the entire set contains 60,000 points. The data were divided into segments that are 2048 points long that were each fit to a line that was subtracted from the original data. This operation ensured proper detrending before any further calculation. Each 2048-point segment was then either Fourier-

transformed in order to obtain 1024 points in the frequency domain or averaged in a root mean square fashion to obtain the overall power. These results were averaged across all the segments. This allowed the calculation of an average and a standard deviation for the overall power as well as power across all frequencies. In order to keep the noise signal on the same order of magnitude as the voltage values, the power spectra are presented in $V/\sqrt{\text{Hz}}$ scale (i.e. the magnitude of the complex number in the frequency domain).

Afterwards, the noise power overall and at 1 Hz were plotted as a function of cycle number. The standard deviations are plotted as error bars on the total power. For clarity, the error bars are not displayed in the other presentations.

In order to calculate the histograms, data were again divided into 2048-point-long segments, which were fit to a line that was subtracted from the said segment. The entire signal was then reconstructed in order to achieve a time trace that shows the noise free of any background trends. This signal was then turned into a histogram by employing 128 bins between $-60 \mu\text{V}$ to $60 \mu\text{V}$ and counting the number of voltage points that fell into each bin. These data were visualized by plotting the number of members at each bin vs. the center of the bin.

The analyses were performed under Python-based in-house written software employing SciPy and NumPy packages operating under SPyDer development environment.

Acknowledgment

Funding from TÜBİTAK is gratefully acknowledged under Project 115C122.

References

1. Barker, G. C. *Electroanal. Chem. Inter. Electrochem.* **1969**, *21*, 127-136.
2. Blanc, G.; Gabrielli, C.; Keddam, M. *Electrochim. Acta* **1975**, *20*, 687-689.
3. Hladky, K.; Dawson, J. L. *Corr. Sci.* **1980**, *21*, 317-322.
4. Mansfeld, F.; Xiao, H. *J. Electrochem. Soc.* **1993**, *140*, 2205-2210.
5. Legat, A.; Doleček, V. *J. Electrochem. Soc.* **1995**, *142*, 1851-1859.
6. Roberge, P. R.; Lenard, D. R.; *J. Appl. Electrochem.* **1998**, *28*, 405-410.
7. Cottis, R. A. *Corrosion* **2001**, *57*, 265-286.
8. Aballe, A.; Bethencourt, M.; Botana, F. J.; Marcos, M. *Electrochem. Comm.* **1999**, *1*, 266-270.
9. Cottis, R. A.; Homborg, A. M.; Mol, J. M. C. *Electrochim. Acta* **2016**, *202*, 277-287.
10. Roberge, P. R. *Corrosion* **1999**, *50*, 502-513.
11. Knott, K. F. *IEEE Electronics Letters* **1965**, *1*, 132.
12. Roberge, P. R.; Beaudoin, R.; Verville, G.; Smit, J. *J. Pow. Sources* **1989**, *27*, 177-186.
13. Martinet, S.; Durand, R.; Ozil, P.; Leblanc, P.; Blanchard, P. *J. Pow. Sources* **1999**, *83*, 93-99.
14. Baert, D. H. J.; Vervaeet, A. A. K. *J. Pow. Sources* **2003**, *114*, 357-365.
15. Martemianov, S.; Adiutantov, N.; Evdokimov, Yu. K.; Madier, L.; Malliard, F.; Thomas, A. *J. Sol. State Electrochem.* **2015**, *29*, 2803-2810.
16. Motchenbacher, C. D. *Low Noise Electronic System Design*; John Wiley and Sons: New York, NY, USA, 1993.
17. Mansfeld, F.; Sun, Z.; Hsu, C. H.; Nagiub, A. *Corros. Sci.* **2001**, *43*, 341-352.